Simulation of Action Potential and Wake Trigger Processes in MATLAB Environment

Murat Beken*‡, Önder Eyecioğlu*, Batuhan Hangün**, Nursaç Kurt***

* Department of Computer Engineering, Bolu Abant İzzet Baysal University, BOLU

**Independent Researcher, İSTANBUL

***Department of Software Engineering, İstinye University, İSTANBUL

(murat.beken@ibu.edu.tr, onder.eyecioglu@ibu.edu.tr, batuhanhangun@gmail.com, nursackurt96@gmail.com)

‡Department of Computer Engineering, Bolu Abant İzzet Baysal University, BOLU, Turkey, Tel: +0374 254 10 00

murat.beken@ibu.edu.tr

Received: 06.01.2022 Accepted:30.03.2022

Abstract- Even though, distance education based on Web services has its benefits in terms of both economic and academic, some specific fields are still in need of an appropriate adaptation to make them more suitable for distance education. Fields like engineering and natural sciences that rely on experiments and implementations are some of the most important examples of them. As a result, many studies have focused on creating virtual laboratories which make it possible to make experiments remotely by using digital devices like computers. In our study, we aimed to simulate the action potentials in MATLAB's Simulink environment. Second, a MATLAB GUI was designed to create a more user-friendly interactive environment. For the simulations, two different observations have been done. One for the constant current and one for the varying current. In those tests, forward and reverse action potentials were observed. Results were compared with the results from physical experiments. This study shows that virtualization of electrical circuit experiments is easy to implement, and the resultant virtual test environment has good usability and fidelity to the physical test environment.

Keywords Action potential, simulation, wake trigger, MATLAB, Simulink, distance education.

1. Introduction

Distance education has become one of the standards in today's educational system. As a result, the goal of designing virtual laboratories for STEM students is very important to create a learning environment that feels and benefits the same way as real-world laboratories. In one of the earliest studies in the virtualization process, Kuo et al. designed a web-based virtual laboratory to carry out some experiments that are required in the syllabus of an undergraduate course on communication principles at the National University of Singapore (NUS). The study showed that without having to purchase expensive spectrum analyzers, students could have easily carried out the required experiments by using virtual laboratory equipment [1]. In Wolf's study in 2010, student learning was assessed in a virtual laboratory environment that is designed to teach students the network systems. The findings demonstrate that not only do people learn in labs, but they also learn (45.9%) almost as much as they do in lectures (54.1%). Virtual laboratories have also been shown to assist students with prior networking knowledge [2]. Another example by Hawkins and Phelps addresses the usage of a virtual laboratory at a general chemistry course. In the given study, students were separated into two groups. The first group has consisted of students which attend actual in-place laboratories, and the other is consisted of those who attend virtual laboratories. Results have shown that there were no significant differences in scores on the tests taken after the course [4]. In a more recent study by Kapilan, Vidhya, and Gao, mechanical engineering students have attended a fluid mechanics virtual laboratory during the COVID-19 quarantine. More than 90% of the participants in their research were pleased with the virtual laboratory, and they stated that the virtual laboratory exercises helped their learning process. They also believed that the virtual laboratories may be used until the COVID-19 pandemic problems were resolved [5].

The cell membrane isolates the biologically active intracellular space electrically and mechanically from the surrounding environment. It concentrates functional units, biologically relevant molecules, and structures and thus made it possible to develop life. Additional functionality is given to it by a variety of proteins embedded in it. As an electrical insulation layer, the cell membrane enables the establishment of an electrical voltage potential between intra- and extracellular space, which provides the energy for many biological processes. The structure and adjustment of the potential are carried out by a group of proteins, which include

the ion channels that form nanometer-sized pores in the cell membrane and transport passively or actively charged particles. Due to the high electrical resistance of the cell membrane and the low thickness of a few nanometers, the potential in it causes an enormously high electric field of approximately 107 V/m. It is therefore not surprising that many of the membrane proteins have a function sensitive to membrane tension. The membrane itself also has potential-dependent physical properties such as its intrinsic mechanical stress [6]. The highly sensitive patch-Clamp-technique allows to determine the electrical voltage of a cell or membrane piece in any way and to measure the resulting charge flows so precisely that currents can be determined by individual ion channels. This makes it possible to artificially stimulate the function of potential-dependent proteins. In combination with the technique of high-precision force spectroscopy, which detects forces in an order of magnitude relevant to individual proteins, the electrical and mechanical properties of proteins can be stimulated very decisively and measured simultaneously precisely.

In this study, we aimed to model and simulate the action potential and wake trigger processes of the nerve cells by using MATLAB and Simulink to create a virtual tool that can be used as laboratory equipment in virtual laboratories in distance education.

2. Materials and Method

Action potentials are rapid, short-term changes of the membrane potentials on nerve cells. They are used for arousal transmission in the body.

Measuring the action potential to measure the action potential, an axon at a certain point with different voltages electrically irritated. At a slightly remote location, the reaction of the axon is measured using electrodes and the oscilloscope (Fig. 1).

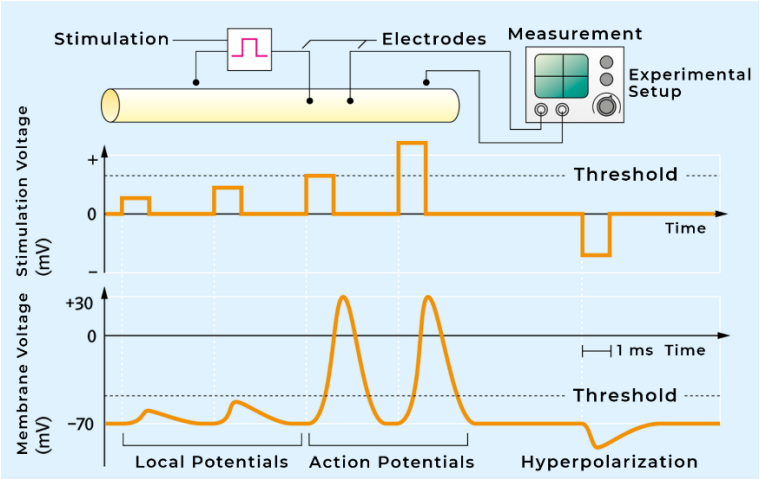

Fig. 1. Irritant strength and membrane potential (Adapted from [10]).

A positive irritant tension leads to a short-term local increase in membrane potential. The higher the irritant voltage, the higher the change in membrane tension, the depolarization. If this exceeds a certain threshold, the membrane potential changes abruptly within a millisecond up to a peak value of approx. +30 mV. The axon actively forms an action potential that spreads and propagates via the axon [7]. After exceeding the voltage threshold, a rapid, strong increase in potential is measured in the depolarization phase (Fig. 2).

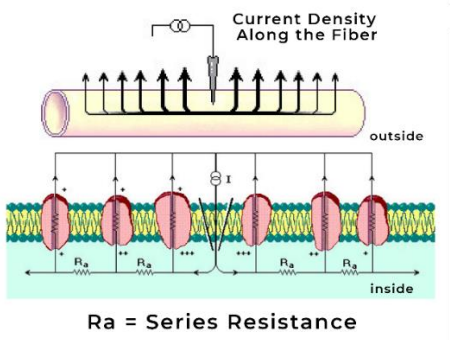

Fig. 2. Action potential (Adapted from [10]).

The course of action potential graph consists of the following steps:

1) Rest potential: Before the start of an AP, the sodium channels are closed and can be activated.

2) Threshold

3) Depolarization: During this time, the activation Gates open Sodium channels are then open and activated. If a stimulus arrives, it will some sodium channels open. This is done by changing the conformation of the charged amino acids in response to the change in voltage when the stimulus is added. If the channels are now open, sodium ions flow in the charge gradient following inwards since the inside of the cell is negative compared to the outside.

4) Repolarization: Now the inactivation gates of the sodium channels slowly close that are then closed and activatable. At the same time, the potassium

channels open. Therefore, potassium flows outwards to avoid the negativity that prevails in their balance.

After a short time, the potential in the repolarization phase decreases again to the resting potential. Action potentials always show the same course. Both the duration of each phase and their electrical potential are always the same; they happen this way or not at all. This is called the all-or-nothing law. If the irritant electrode temporarily results in a more negative voltage than the resting potential, the membrane voltage drops below the rest ingenuity voltage (hyperpolarization) at the measuring point [8].

2.1. Molecular Processes

A change in the membrane potential can be explained by a change in the ion concentrations on the inside and outside of the axon membrane. Alan Hodgkin and Bernard Katz conducted experiments in which they replaced the Na+ ions outside the axon with positively charged but much larger ions for which the axon membrane is not permeable [9]. No action potentials could be triggered in this experimental arrangement. The researchers hypothesized that the action potential is created by opening Na+ ion channels and the rapid influx of Na^+ ions into the axon.

Measurements showed that the external concentration of Na^+ ions is 10 times higher than the internal concentration. The hypothesis was confirmed by patch-clamp-messing: During depolarization, many Na^+ ion channels are open, but only a few K^+ ion channels [9,10]

2.2. The Patch Clamp Technique

With this technique, it is possible to investigate when ion channels are open or closed (see edge column). The ion current is measured on a very small membrane surface. A micropipette made of glass is attached to the cell membrane by light suction. This delimited part of the axon is so small that individual ion channels can be analyzed. The glass capillary is filled with a saline solution that conducts the current. A second capillary is inserted into the cell [11]. When measuring the current flow, one observes sudden, short-term jumps. The channel opens, ions diffuse through then the channel closes again. In this way, the number of ions can be measured in a certain period. To investigate which ions, move through the ion channels, sodium ion channels or potassium ion channels can be specifically blocked [12,20].

Ion currents at the ion channels in the membrane of an axon, voltage-controlled Na^+, and K^+ ion channels are present in sufficient density. The axon is depolarized by an electrical stimulus (Fig. 5a). This opens a few Na^+ ion channels. The opening of the first channels leads to increased depolarization, which leads to a further opening of Na^+ ion channels. At the threshold of approx. -50 mV, all available Na+ ion channels in the environment of the depolarized axon membrane suddenly open. Na^+ ions flow in large numbers into the interior of the axon [13]. The proportion of positively charged ions thus decreases outside the axon, within larger. This results in the membrane potential becoming positive within one millisecond (Fig. 3).

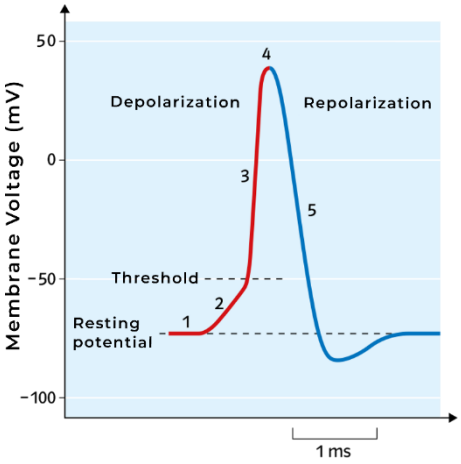

Fig. 3. A course of action potential (Adapted from [12]).

The individual Na^+ ion channels close spontaneously after approx. 2 ms. Hereby getting no more Na^+-ions into the axon and the potential does not increase any further. The closed Na^+-ion channels are then inactivated for a short time and cannot be opened (refractory time) [9]. Only after a few milliseconds do they become activated again. The refractory time limits the number of triggerable action potentials (frequency) and determines the propagation of action potentials in only one direction. The repolarization of the axon membrane (Fig. 5b) is mainly caused by the outward current of K^+ ions [10]. Due to the increased outflow of the K^+ ions from the axon, the cell interior becomes more negative until the resting potential is reached. Only then do the K^+ ion channels close again.

Fig 4. describes the operations on the Na^+ ion channels using the text and Fig. 5 and explains how the phases of the action potential occur in Fig. 3.

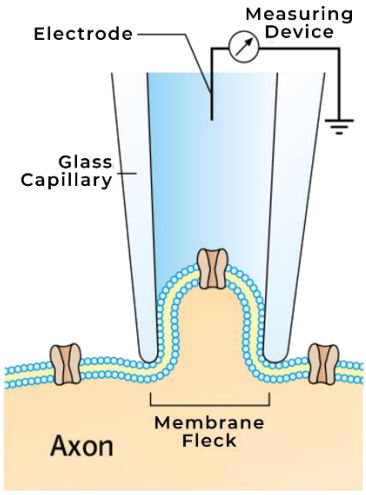

Fig. 4. Patch-Clamp Technique (Adapted from [12]).

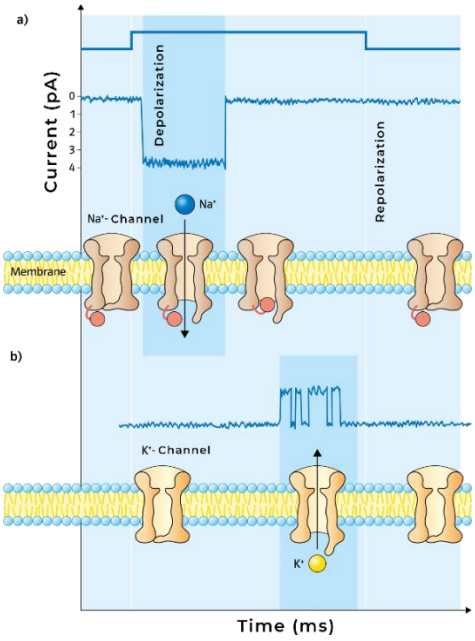

Fig. 5. Processes on the ion channels during an action potential (Adapted from [12]).

2.3. Nonlinear Capacity (NLC)

Membrane proteins, which have a voltage-hanging property, require a corresponding electrically charged sensor domain. This voltage sensor moves due to a potential change in the electric field and causes a conformation change of the protein. If such charge movements are induced at a change in the transmembrane voltage, they add up to the normal capacitive current of the membrane. In this case, it is referred to as tor stromen (gating currents), which for the first time were called C. M. Armstrong and F. Bezanilla could be detected using voltage-controlled sodium channels using the Voltage-Clamp technique [7]. The capacitation of the membrane in which such proteins are embedded is thus also voltage-hanging.

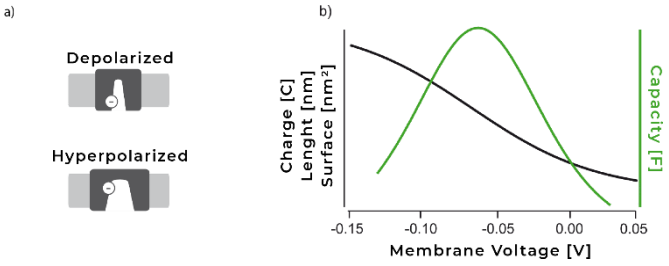

Fig. 6 Prestin and his nonlinear Capacity (Retrieved from [8]).

If a cell or its membrane (light grey) is depolarized, the Prestin molecules (dark grey) are preferably in their compact state (a). In hyperpolarization, they change to a more extensive state (longer, more area). The sensor for this conformation change is a charged domain (assumed here as negative) of the Prestin molecule, which moves within the membrane because of the changed potential - equivalent to a charge current. The behavior in the ensemble (b) therefore has an electrical signature in the form of a nonlinear capacity dependent on the voltage (Eq. 3). The sizes of the moving charges and geometric changes show a sigmoidal behavior (Eq. 4).

A very simple model in the case of Prestin assumes that there are two states: a compact (depolarization) and an expanded (hyperpolarization), each of which requires different sized membrane surfaces (Fig. 6). If one considers only the different electrical energies of the two states, one can describe the probability of which state a molecule is in with the help of a simple Boltzmann factor [14]. In these, the size of the moving sensor charge e. If the sensor charge only moves through a part of the electric field, i.e., not through the entire membrane, the sensor charge in the conformation change is reflected accordingly in the size of z. In an ensemble of molecules, the total charges in a state can be summed up to a total charge Q. The greeting of Q is now dependent on the diaphragm voltage V and can be described by a two-state Boltzmann function:

$$Q(V) = \frac{Q_{max}}{1 + e^{-\frac{V - v_h}{a}}} \tag{1}$$

With the maximum charge shift Q_{max}, the half-value voltage V_h and where k_B is the Boltzmann constant, T the temperature, and e the elementary charge. The first derivation of the formula (Eq. 1) to V then gives, considered the non-voltage-dependent membrane capacity C_0, the relationship between the capacity C and the voltage V.

$$a = \frac{k_B T}{ze} \tag{2}$$

$$C(V) = C_0 + Q_{max} \frac{e^{-\frac{V - V_b}{a}}}{a\left(1 + e^{-\frac{V - V_h}{a}}\right)} \tag{3}$$

This very simple model provides a connection that already describes the measured data very well [15]. It should be noted that in the context of equation (3) C_0, C_M is mentioned below. The typical form of the voltage-dependent capacity and the corresponding charge shift are shown in Fig. 6. If in a particular experiment, a property L of the cells is missing, which is directly coupled with the conformation change, such as the change in length of the outer hair cells, the stress dependence can also be described according to the relationship of Eq. 1:

$$L(V) = \frac{L_{max}}{1 + e^{-\frac{V - V_h}{a}}} \tag{4}$$

3. Simulation of Nerve Cells with the Help of Electronic Components

In the following experiments, we now want to apply all the results and findings to the biological situation of a nerve cell. For this purpose, a biological membrane is simulated using electronic components, and we are studying how electrical signals are transported through this nerve membrane.

When constructing the model, two properties of the membrane must be considered:

The membrane of a nerve cell separates the inside of the cell from the outside. On both sides of the membrane, there is electrolyte liquid, i.e., an electrical conductor [16]. The double lipid layer of the membrane isolates the outside of the membrane from its inside. Such an arrangement behaves like a capacitor: on both sides of the insulator (in the case of the membrane: double lipid layer), electric charges of different signs can be stored, and the insulator prevents them from balancing each other by current flow. As with the capacitor, the "storage capability" of the arrangement is also called capacitance (membrane capacitance C) [16]. We simulate the double lipid layer of the membrane through an electrical capacitor of capacitance 0.47 µF.

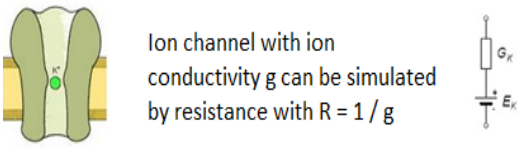

Fig. 7. Ion channel and electronic simulation (Adapted from [16]).

However, we need another electrical building block for our simulation: The electrolytes inside and outside the cell are not completely isolated from each other by the membrane. Through passive (constantly opened) ion channels, which are stored in the membrane (Fig. 7), ions and thus electrical currents can flow through the membrane [16]. The electrical properties of ion channels (i.e., the parallel connection of a variety of ion channels on a small membrane section) can be described by electrical resistance. We, therefore, add a 2.2k resistor to the circuit. It connects the inner side to the outer side of the membrane.

3.1. Temporal change in membrane potential, formation of arousal

The first circuit seen in Fig.8 is designed on MATLAB Simulink and given by Fig. 9. The waveform of the output signals can be viewed by using Simulink scopes.

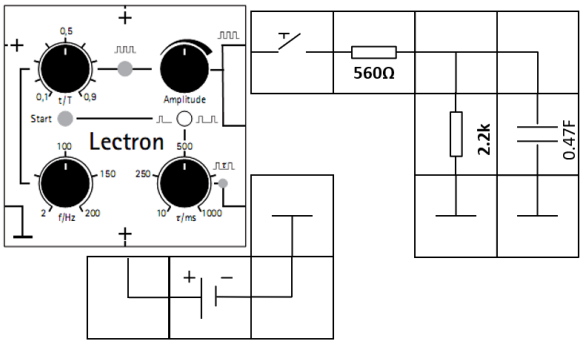

Fig. 8. Circuit 1 (Retrieved from [16]).

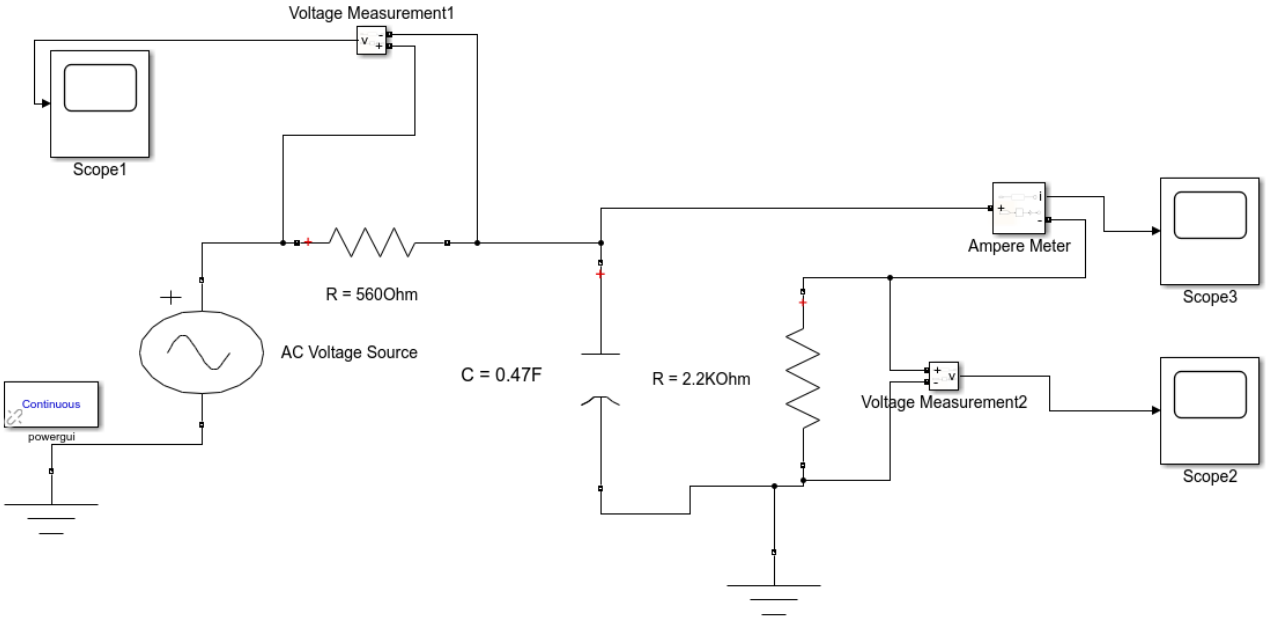

Fig. 9. Simulink representation of Circuit 1 (Adapted from [16]).

3.2. Spatial propagation of signals

Secondly, an elongated cell model (Fig. 10) was designed and created (Fig. 11). Two RC connections have been added to Circuit 1. 560 Ω resistors simulate longitudinal resistance across the membrane.

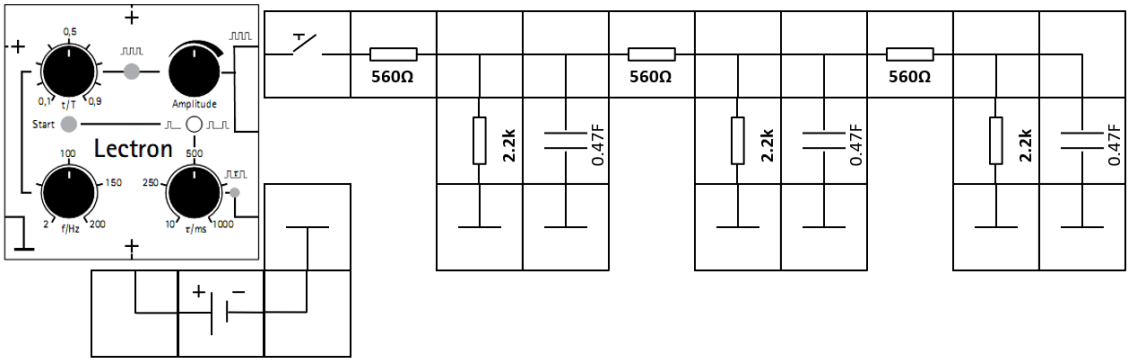

Fig. 10. Circuit 2 (Retrieved from [16]).

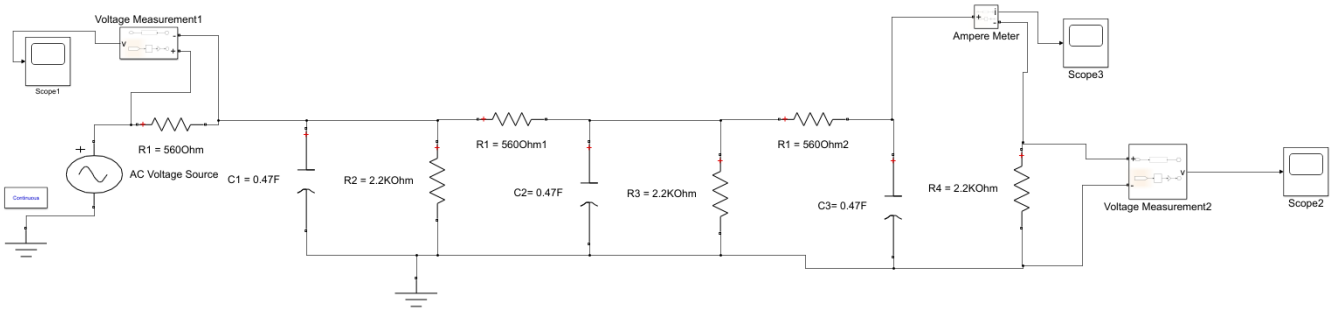

Fig. 11. Simulink representation of Circuit 1 (Adapted from [16]).

In addition to Simulink design, a GUI was also created to display the results and effects more appealingly. Figs. 12-13 are from the designed MATLAB GUI. Presented GUI allows users to visualize the effects of certain parameters.

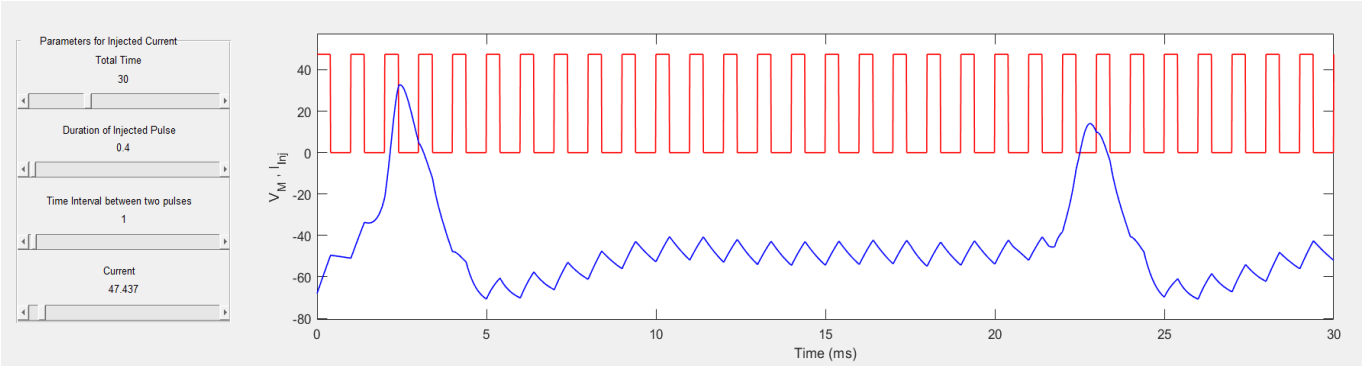

Fig. 12. A screenshot from the MATLAB GUI is designed to visualize the effects of certain parameters.

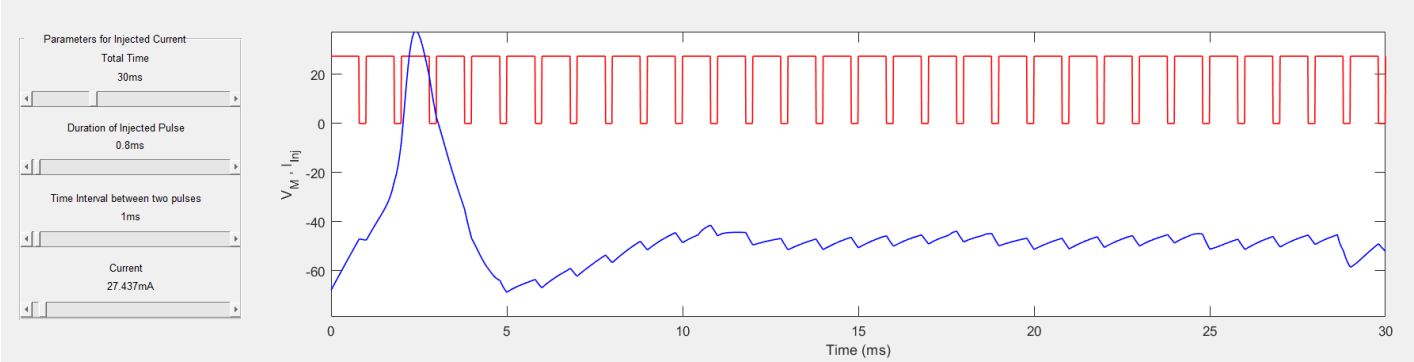

Fig. 13. A screenshot from the MATLAB GUI is designed to visualize the effects of certain parameters.

By using a constant action current of 47 mA in the designed Simulink circuit, the change of forward and reverse action potentials for different triggers was observed. While the difference in forward and reverse action potentials is high at low action current values, it is seen in Fig.14 that the difference decreases as the current value increases.

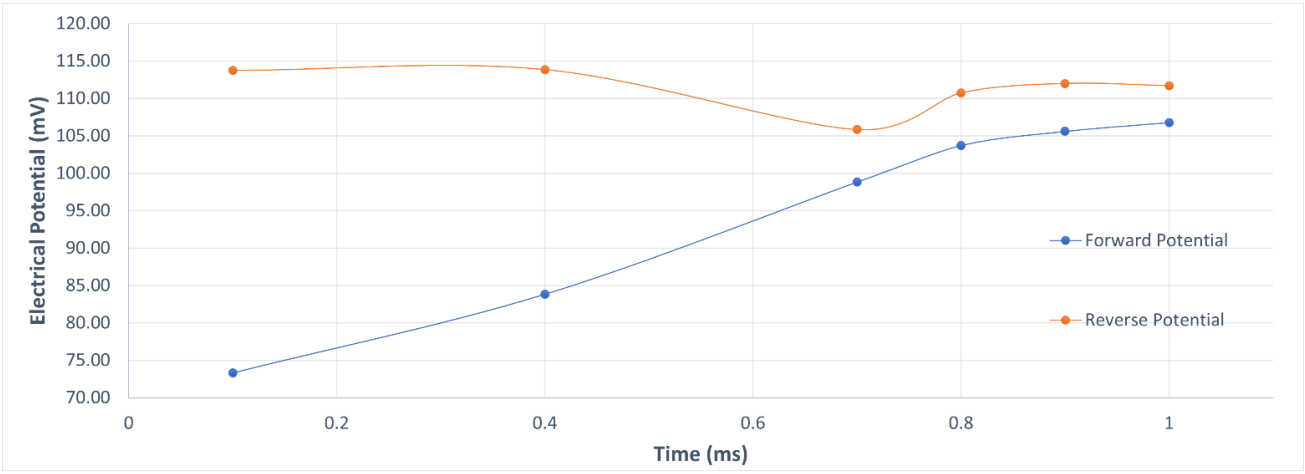

Fig. 14. Change of forwarding and reverse potentials according to constant electric current of 47 mA.

Another observation was made over the changing action currents at a fixed point in time. Fig. 15 shows that the forward and reverse action potentials produced in response to the action currents with 17 mA, 27 mA, 37 mA, 47 mA, and 62 mA values change proportionally depending on the increasing current value.

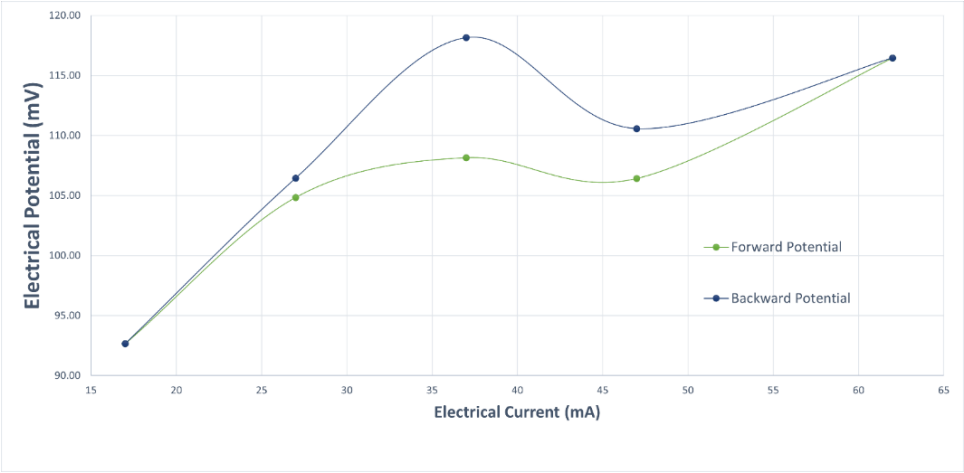

Fig. 15. Change of forwarding and reverse potentials according to varying electric current.

4. Conclusion

Simulations of action potentials of nerve cells are very important in biomedical studies. Such simulations are normally done with physical laboratory equipment in a physical laboratory. In this study, we aimed to digitally simulate the action potentials of nerve cells. The main reason behind this was the rising importance of virtualization of the physical laboratories that emerges with the current remote working and distance education trends. For this task, we used MATLAB and Simulink to create two different test environments. The first one is a Simulink-based electrical circuit representation of the action potentials, and the second one is a GUI-based, more interactive representation. To see the correctness of the models, two tests were done. One is a test to calculate the action potentials under a constant current, and the other is to calculate them under a varying current. Simulation results have been compared with the results from the physical setup, and the results are compatible with each other. This study suggests that virtualizing electrical circuit experiments is simple to do, and the resulting virtual test environment is both practical and consistent with the physical test environment.

Acknowledgements

This work is supported by Nişantaşı University Scientific Research Projects Coordination Unit (Project no: BAP00022).

References

[1] C. C. Ko et al., "A web-based virtual laboratory on a frequency modulation experiment," in IEEE Transactions on Systems, Man, and Cybernetics, Part C (Applications and Reviews), vol. 31, no. 3, pp. 295-303, Aug. 2001, doi: 10.1109/5326.971657.

[2] T. Wolf, "Assessing Student Learning in a Virtual Laboratory Environment," in IEEE Transactions on Education, vol. 53, no. 2, pp. 216-222, May 2010, doi: 10.1109/TE.2008.2012114.

[3] I. Hawkins and A. J. Phelps, “Virtual laboratory vs. traditional laboratory: which is more effective for teaching electrochemistry?” Chemistry Education Research and Practice, vol. 14, no. 4, pp. 516–523, Jul. 2013.

[4] I. Hawkins and A. J. Phelps, “Virtual laboratory vs. traditional laboratory: which is more effective for teaching electrochemistry?,” Chemistry Education Research and Practice, vol. 14, no. 4, pp. 516–523, Jul. 2013.

[5] N. Kapilan, P. Vidhya, and X.-Z. Gao, “Virtual Laboratory: A Boon to the Mechanical Engineering Education During Covid-19 Pandemic,” Higher Education for the Future, vol. 8, no. 1, pp. 31–46, Dec. 2020.

[6] J. Yalcinkaya, F., and Unsal, H. Matlab/Simulink Based Comparative Analysis of the Effect of Ion Concentration on Action Potential by Using Hodgkin-Huxley and Morris-Lecar Neuron Models. In 2017 21st National Biomedical Engineering Meeting (BIYOMUT) (pp.i-iv). IEEE.

[7] C. M. Armstrong and F. Bezanilla, “Charge Movement Associated with the Opening and Closing of the Activation Gates of the Na Channels,” Journal of General Physiology, vol. 63, no. 5, pp. 533–552, May 1974, doi: 10.1085/jgp.63.5.533.

[8] J. F. Ashmore, “Forward and reverse transduction in the mammalian cochlea,” Neuroscience Research Supplements, vol. 12, pp. S39–S50, Jan. 1990, doi: 10.1016/0921-8696(90)90007-p.

[9] A. L. Hodgkin and A. F. Huxley, “A quantitative description of membrane current and its application to conduction and excitation in nerve,” The Journal of Physiology, vol. 117, no. 4, pp. 500–544, Aug. 1952, doi: 10.1113/jphysiol.1952.sp004764.

[10] Ernst Klett Verlag, Natura Biologie Oberstufe/Themenband Ökologie Ausgabe ab 2016. Stuttgart Klett, 2018.

[11] I. S. Edelman and S. G. Schultz, Annual review of physiology. Vol. 41, 1979. Palo Alto, Calif.: Annual Reviews Inc, 1979.

[12] K. S. Cole, “Mostly Membranes,” Annual Review of Physiology, vol. 41, no. 1, pp. 1–23, Oct. 1979, doi: 10.1146/annurev.ph.41.030179.000245.

[13] E. K. Verlag, GmbH, Stuttgart 2018 | www.klett.de | Alle Rechte vorbehalten Von dieser Druckvorlage ist die Vervielfältigung für den eigenen Unterrichtsgebrauch gestattet. Die Kopiergebühren sind abgegolten. Die Entstehung des Aktionspotentials, (Lecture note)

[14] E. Neher and B. Sakmann, “Single-channel currents recorded from membrane of denervated frog muscle fibres,” Nature, vol. 260, no. 5554, pp. 799–802, Apr. 1976, doi: 10.1038/260799a0.

[15] J. Santos-Sacchi, S. Kakehata, and S. Takahashi, “Effects of membrane potential on the voltage dependence of motility-related charge in outer hair cells of the guinea-pig,” The Journal of Physiology, vol. 510, no. 1, pp. 225–235, Jul. 1998, doi: 10.1111/j.1469-7793.1998.225bz.x.

[16] J. Santos-Sacchi, “Reversible inhibition of voltage-dependent outer hair cell motility and capacitance,” The Journal of Neuroscience, vol. 11, no. 10, pp. 3096–3110, Oct. 1991, doi: 10.1523/jneurosci.11-10-03096.1991.

[17] Physics-Praktikum for students of medicine (Lecture note)

[18] W. von Engelhardt and G. Breves, “Physiologie der Haustiere,” Schweizer Archiv für Tierheilkunde, vol. 147, no. 11, pp. 507–507, Nov. 2005, doi: 10.1024/0036-7281.147.11.507.

[19] A. van Schaik, “Building blocks for electronic spiking neural networks,” Neural Networks, vol. 14, no. 6–7, pp. 617–628, Jul. 2001, doi: 10.1016/s0893-6080(01)00067-3.

[20] B. Tahayori and S. Dokos, “Optimal stimulus current waveshape for a hodgkin-huxley model neuron,” 2012 Annual International Conference of the IEEE Engineering in Medicine and Biology Society, Aug. 2012, doi: 10.1109/embc.2012.6346998.

[21] S. Kirigeeganage, D. Jackson, J. M. Zurada and J. Naber, "Modeling the bursting behavior of the Hodgkin-Huxley neurons using genetic algorithm based parameter search," 2018 IEEE International Symposium on Signal Processing and Information Technology (ISSPIT), 2018, pp. 470-475, doi: 10.1109/ISSPIT.2018.8642781.